Numerical Methods in Geotechnical Engineering, Mestat (ed.) 2002, Presses de l'ENPC/LCPC, Paris

DISCRETE ELEMENT MODELING FOR IRREGULARLY-SHAPED SAND GRAINS

LA MODÉLISATION AUX ÉLÉMENTS DISCRETS D'UN SABLE A GRAINS DE FORME IRRÉGULIÈRE

T. Matsushima[1], H. Saomoto[1]
[1]*Institute of Engineering Mechanics and Systems, University of Tsukuba, Tsukuba, Japan*

ABSTRACT. A simple algorithm for discrete element modeling of complicated grain shapes is presented and evaluated in this paper. Each grain's shape is assumed to be represented by combining several primitive elements (circles in 2-D and spheres in 3-D) suitable for Discrete Element simulation. The proposed dynamic optimization algorithm enables us to obtain the sizes and the locations of the primitive elements so that the best accuracy possible is attained in the modeling. Application of the 2-D Toyoura sand model into a DEM element test is presented and the effect of a grain's shape on the macro behavior of a granular system is discussed.

RÉSUMÉ. Un algorithme simple pour la modélisation par éléments distincts de grains de forme complexe est présenté et évalué dans cette communication. La forme de chaque grain est représentée par une combination de primitives (des circles en 2D et des sphères en 3D) adaptée à la modélisation par éléments distincts. L'algorithme d'optimisation dynamique proposé permet d'obtenir les tailles et la position des éléments de primitives de manière à obtenir la meilleure précision possible dans la modélisation. Une application 2D au sable de Toyoura est présentée, et on discute de l'influence de la forme d'un grain sur le comportement macroscopique du milieu granulaire.

1. Introduction

A rapid increase of computer abilities in the recent past has drastically extended the availability of Discrete Element Method (DEM). Recently, in the field of soil mechanics, some researchers attempted so-called 'virtual' element tests such as a tri-axial compression test with DEM (Thornton and Liu 2000, Muhlhaus, H.-B. et al. 2001). They dealt with a considerable number of 3-D particles (5000 to 10000) to obtain more realistic simulation results. However, it is still difficult to compare such DEM results quantitatively with physical experimental results of real sand mainly because of the lack of adequate grain-shape modeling. Natural sand grains have very complicated shapes necessarily affect the macro behavior (stress-strain curve, dilatancy curve, etc.) of an element test specimen. It seems true to say that angular grains have much higher shear strengths than roundish grains, but the mechanism is still not clear and quantitative estimations have not been successfully made yet.

In order to study this grain-shape effect, several researchers have conducted Discrete element simulations with non-circular (or non-spherical) particles. Rothenberg and Bathurst (1992) conducted a series of bi-axial test with elliptic elements of different aspect ratios and showed that the maximum shear strength was exhibited with a specimen composed of ellipses whose aspect ratio was around 0.8. Mirghasemi et al. (1997) dealt with polygonal particles in order to study the effect of confining pressure on peak shear strength, but grain-shape effects were not disscussed in depth. Matsushima and Konagai (2001) simulated a series of simple shear tests with 2-D elliptic elements and regular polygonal elements to discuss the grain shape effect in detail. It was demonstrated in their study that regular polygonal elements exhibit larger rotational resistance at their contact points, which leads to higher shear strength. They also conducted grain shape analysis for four different sands, and suggested that the mechanism of grain-shape effect of real sands may be similar to that of regular polygonal elements.

In relation to the rotational resistance at the contact points, Iwashita and Oda (1998) proposed a DEM with circular elements in which an additional rotational spring is assumed at each contact point. This is considered as a indirect but efficient approach to include the effect of grain shapes into DEM, though further study between rotational resistance and grain shape is needed.

In an attempt for a 3-D non-spherical element, Lin and Ng (1997) and Ng (1999) proposed the DEM with ellipsoidal elements and Ghaboussi and Barbosa (1990) formulated ployhedron DEM, but they didn't discuss the connection to real grain shapes.

Considering these circumstances, it appeared worth conducting discrete element simulation with grains whose shapes were directly modeled from real sand grains. This study deals with such direct grain-shape modeling by a combination of primitive circular or spherical elements. A newly developed algorithm enables us to find the optimum sizes and positions of primitive elements for describing a complicated grain shape. Its concept is quite simple, and is easily applicable not only in 2-D but also in 3-D modeling. Accuracy and convergence of this algorithm are discussed in detail in this paper. Then the adaptability of the modeled grains into DEM simulations was studied through an element test. Based on the simulation results, the grain-shape effect in such granular materials as sands is then discussed.

2. Dynamic optimization for grain shape modeling

2.1. Basic algorithm

The proposed algorithm is called dynamic optimization; because the optimized solution is obtained through a virtual time-marching scheme. First we assign the number of primitive elements used for the modeling, and set arbitrary initial sizes and locations. Usually the initial size is set to be sufficiently small in comparison with the size of the target grain and the initial locations are assigned inside the target grain. Then, we assume a kind of virtual force acting on the primitive elements. This force is an attraction from the surface of the target grain. The surface of the target grain is given as a set of discrete points, and the attraction directs from the centroid of the primitive element to each surface point (Figure 1(a)(b)). The magnitude of the attraction is proportional to the distance between the primitive element and the surface point.

When plural primitive elements are adopted, it is assumed that the attraction of each surface point acts only on the element closest to the point (Figure 1 (c)). More exactly, the following value δ^{ij} is checked for each element i:

$$\delta^{ij} = d^{ij} - r^{i} \tag{1}$$

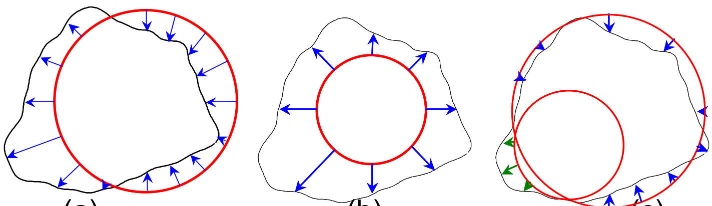

Figure 1 concept of a virtual force acting on the elements

[0] Start
[1] Input of the surface points of a target grain
[2] Calculation of area (volume), gravity center, etc. of the grain
[3] Input the calculation conditions (number of primitive elements, time increment, spring constant, damping coefficient, etc.)
[4] Set the initial sizes and locations of the primitive elements
[5] Iteration loop starts
[6] Loop for each grain-surface point
[7] Detection of the element closest to the surface point
[8] Calculation of virtual force
[9] go back to [6] up to the end of data point
[10] Solve the virtual equation of motion for each element
[11] Calculation of error index
[12] If error index does not reach the threshold, go back to [5]
[13] End

Figure 2 Flow chart of the program

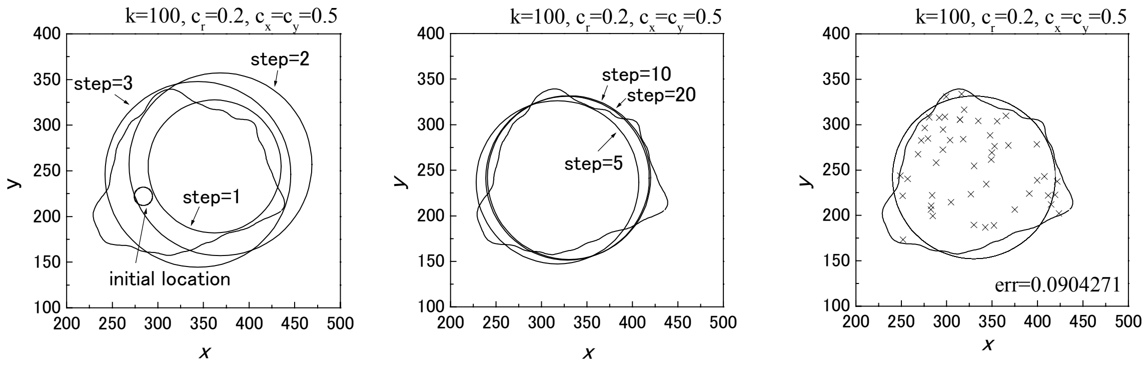

(a) converging process(1) (b) converging process(2) (c) unique solution with various initial positions

Figure 3 an example of the optimization with a single element

where d^{ij} is the distance between j-th surface point and the centroid of i-th element, and r^i is the radius of the element. Then the element which has the minimum δ^{ij} is chosen as the representative element of this surface point, and the following attraction is applied to the element:

$$f^{ij} = k(d^{ij} - r^i) \tag{2}$$

where k is a spring constant. The attraction is directed from the centroid of the element to the surface point when f^{ij} is positive.

By summing all the attractions, each element moves and expands (or shrinks) according to a virtual equation of motion. By introducing an additional damping in the equation of motion, the motion of the elements is converged after some calculation steps. In this converged configuration, the equilibrium has been met in each element for both volumetric and translational components. This final configuration of the elements is then the optimum solution in this algorithm.

The algorithm is summarized in a flow chart (Figure 2).

2.2. 2-D modeling

Figure 3(a)(b) show an example of the 2-D converging process with a single circular element. It is clear that the element approaches to the converged solution with some oscillation. It is necessary to set adequate parameters (spring constant and damping coefficient) for the rapid convergence. Figure 3 (c) shows that a unique solution is obtained wherever the initial position of the element is assigned (cross marks in the figure show the randomly-assigned initial positions).

When plural primitive elements are adopted, however, the converged solution is not unique but is strongly influenced by the initial configuration. Figure 4 shows two different converged solutions that are obtained from 10 different initial configurations with two elements. To judge the accuracy of the converged solution, the following error index is introduced:

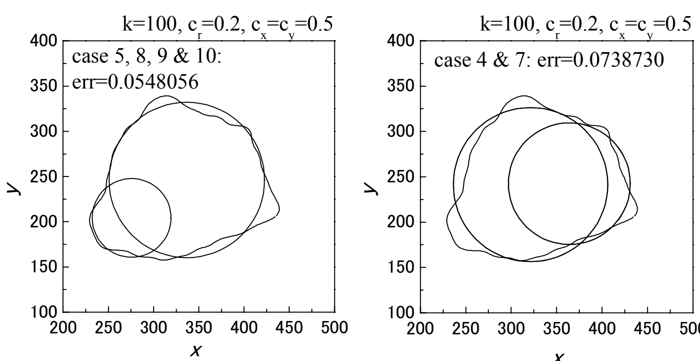

(a) (b)

Figure 4 two solutions obtained with two elements

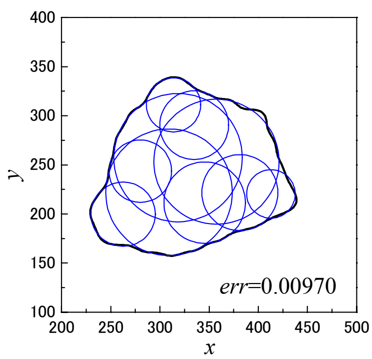

Figure 5 a solution with ten elements

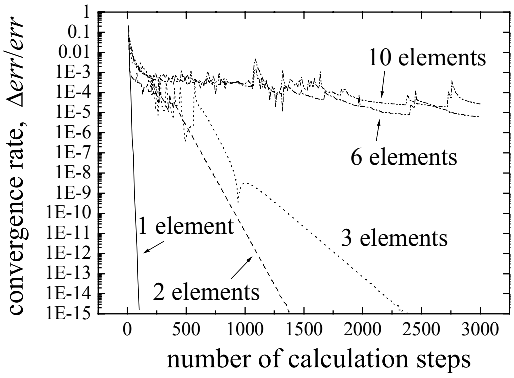

Figure 6 convergence of the calculation

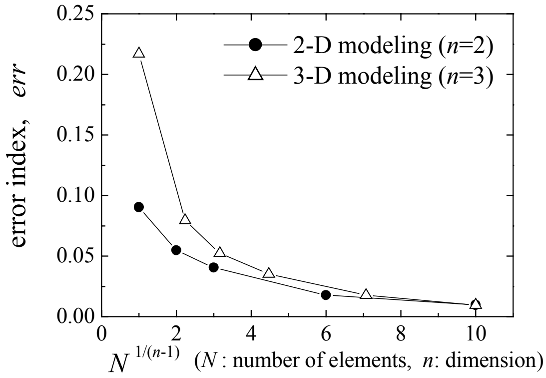

Figure 7 relation between error index and the number of adopted elements

$$err = \frac{1}{N\,R_{eq}} \sum_{j=1}^{N} \left| \bar{d}^{\,j} - \bar{r}^{\,j} \right| \tag{3}$$

where N is the number of surface points ofthe target grain, R_{eq} is the radius of the circle whose area (or volume in 3D) is equivalent to the one of the target grain, $\bar{d}^{\,j}$ is the distance between the j-th surface point and the centroid of the element representing this surface point, and $\bar{r}^{\,j}$ is the radius of the element.

Since it is difficult to find the theoretical optimum solution, we currently repeat a sufficient number of calculations with different initial positions, and the most accurate solution is chosen based on the error index.

When the number of adopted elements is increased, another problem arises; some of the elements come fully inside another element and become inactive. To avoid the degradation of the solution by these inactive elements, it is effective to introduce an additional scheme that such elements are re-located around the most-inaccurate surface point. Figure 5 shows an example obtained with ten elements, which seems to attain sufficient accuracy of overall grain shape. It should be noted that this modeling cannot describe the small surface roughness of real sand grains. However, this surface-roughness effect may be incorporated into DEM simulations by changing the friction coefficient.

Figure 6 shows the convergence with a different number of primitive elements. Convergence becomes worse with larger numbers of elements and the curves are jagged (not monotonic). This is due to the fact that the change of the elements' configurations causes a change of the mathematical problem itself; the connection of virtual springs between the elements and the grain surface points are determined by the current configuration of the elements.

Figure 7 shows the relation between the final error index and the number of the primitive elements. The final error index is determined as the value after a sufficient number of calculation steps. Certainly, a better result is attained with larger number of elements, but the increase of the number of elements leads to the increase of the computation time in DEM simulation. Therefore, an adequate number of elements for the modeling should be chosen taking account of both the accuracy and the computational efficiency in DEM simulation.

2.3. 3-D modeling

It is straightforward to apply the above algorithm into 3-D modeling. However the number of elements required to satisfy a certain accuracy becomes much larger. Figure 8 shows an example of 3-D grain modeling with 100 elements. The obtained error index is *err*=0.00962 which is comparable to that of 2-D modeling with 10 elements (err=0.00970), though the target grain shape is completely different. From a dimensional consideration, the accuracy with *N* elements in 2D is same as that with N^2 elements in 3D. According to Figure 6, the accuracy with smaller elements does not obey this rule, mainly due to the difference of the target grain shape, but the accuracy with a larger number of elements seems to be in good agreement with the rule.

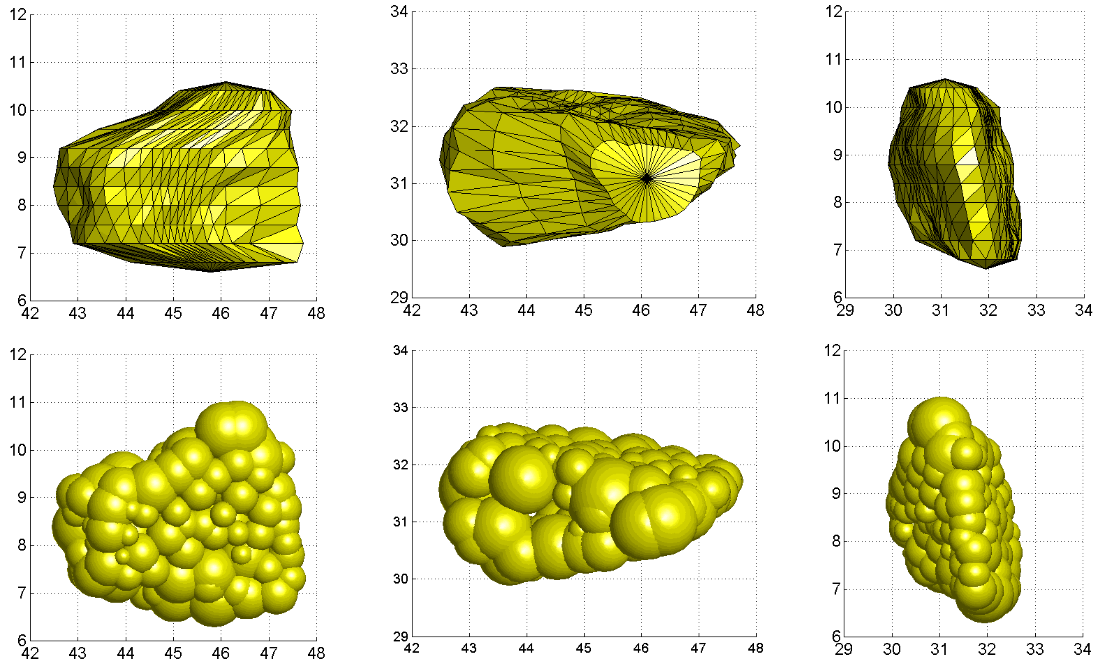

(a) x-z plane (b) x-y plane (d) y-z plane

Figure 8 an example of 3-D modeling
(top: original surface data, bottom: model with 100 spheres)

Therefore we can choose the number of primitive elements used for the representation of one grain based on Figure 6

3. Application to Discrete Element Method

3.1. 2-D Modeling of Toyoura sand

Recent developments of digital microscopes enable us to easily obtain the shape of sand grains, and some research has been done on grain shape analysis of various sands using this technology (Yoshida 1993, Matsushima and Konagai 2001). However only 2-D images as shown in Figure 9 were dealt with, and a 3-D grain-shape detection system has not been established yet. In this study we also limit the discussion to 2-D modeling.

Figure 9(a) shows a part of a grain shape catalog of Toyoura sand, a commonly-used sand in Japan. 50 grains are detected in this study and each grain was modeled with 10 circular elements. Size distribution of these grains is plotted in Figure 10. It seems to be reasonable in comparison

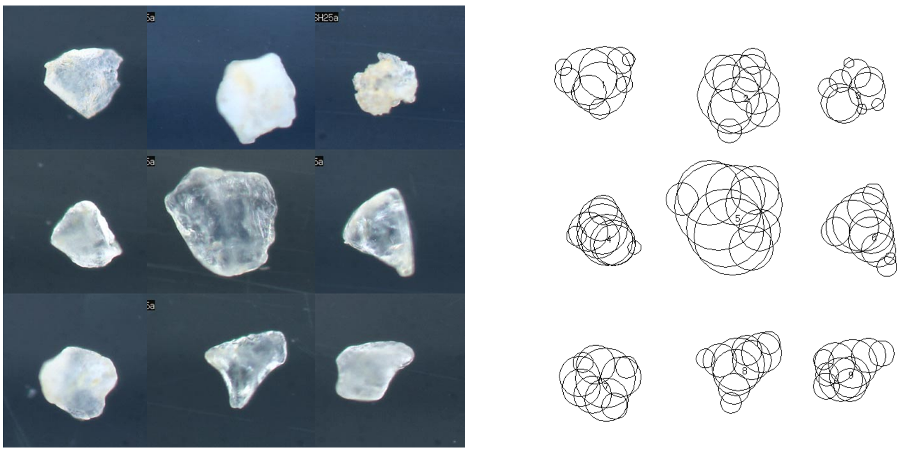

(a) original grain images (b) grains modeled with ten circles

Figure 9 2-D grain catalog of Toyoura sand

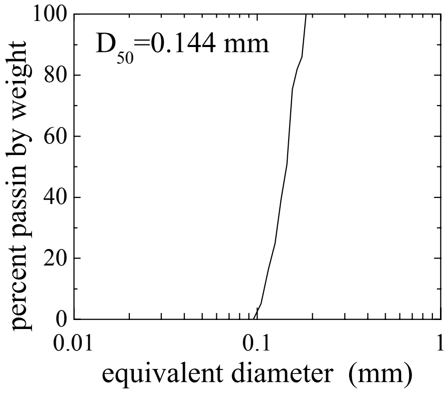

Figure 10 size distribution

Table 1. DEM parameters used in this study

density of grain	2.64 (g/cm^2)
spring constant (normal)	1.0e9 (g/s^2)
spring constant (shear)	2.5e8 (g/s^2)
damping coefficient (normal)	2.0e2 (g/s)
damping coefficient (shear)	1.0e2 (g/s)
friction coefficient	27 (deg.)
time increment	5.0e-8 (s)

with that obtained by usual sieving process.

The DEM program used in this study was developed by Matsushima (2001), and it allows combining a certain number of primitive elements in rigid way. In other words, the contact judgment and the calculation of contact forces are conducted for each primitive element, and the equation of motion is solved for each grain. It should be noted that the catalog of Toyoura sand model constructed in this study can also adapted to DEM, which allows combining some primitive elements with additional springs.

DEM parameters used in the simulation are listed in Table 1.

3.2. Numerical example

A bi-axial test with rigid sidewalls was simulated. The number of grains was 1000, meaning that each 50 grains was duplicated 20 times and was randomly located. The initial specimen was 2.97mm wide and 5.98mm high and the initial void ratio was set to 0.201 (dense). Both side walls were programmed to move so as to keep the total reaction force constant (5.98e6 g mm/s^2). Since the height of the specimen was reduced due to loading, the confining pressure gradually changed (1.0kN/m at the initial state and 1.2kN/m at the final state with an axial strain of 16.7%).

Figure 11 shows the snapshots of the specimen before and after axial compression. Figures 12 and 13 show the evolution of the mobilized friction angle and the volumetric strain (dilatancy relation), respectively. In the figures the result by an equivalent circles model (whose volume

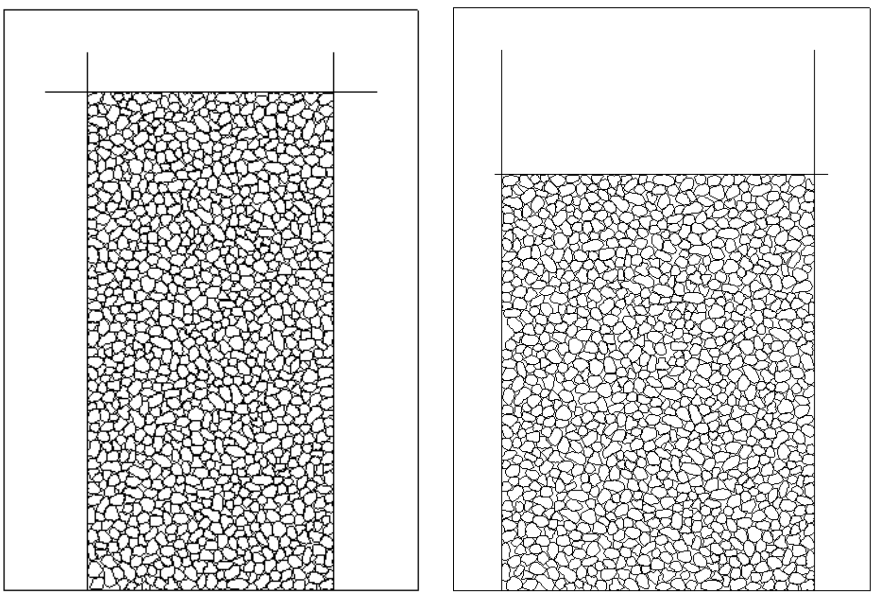

(a) before compression (b) after compression (axial strain=16.7%)

Figure 11 bi-axial test with 1000 Toyoura sand grains

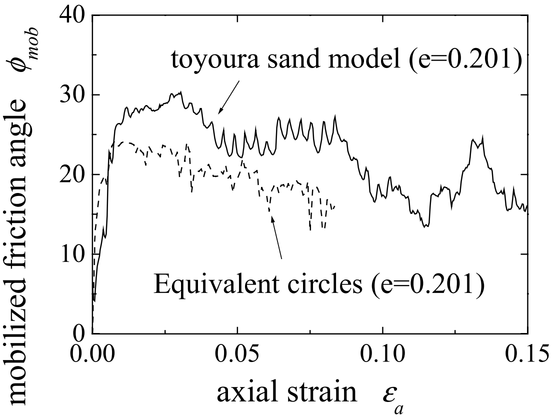

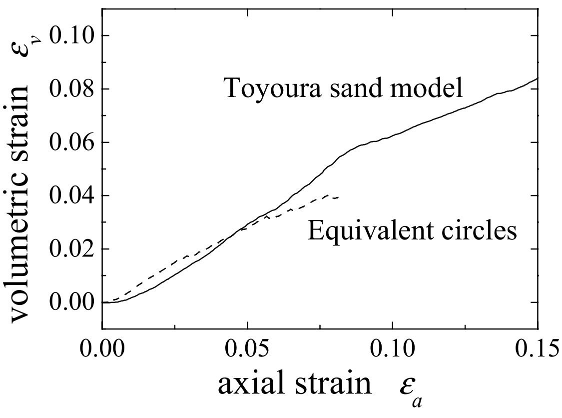

Figure 12 evolution of mobilized friction angle

Figure 13 evolution of volumetric strain

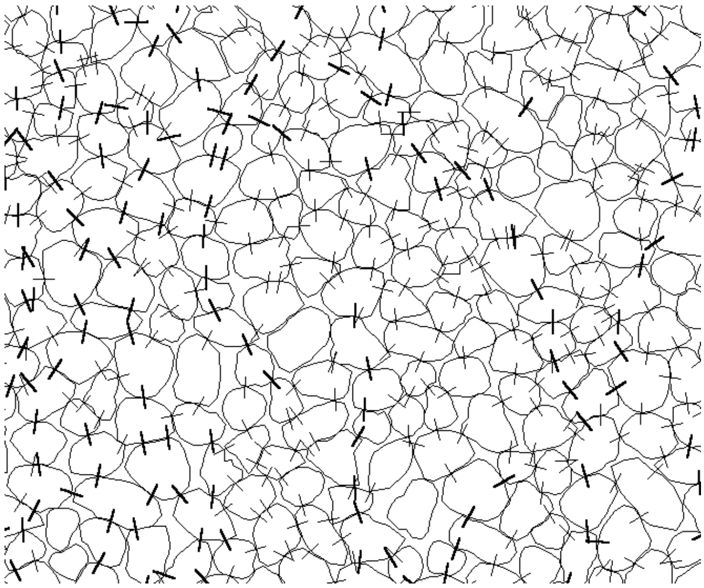

Figure 14 granular columns formed in the compressed specimen

distribution is exactly equal to the Toyoura sand model) is also plotted. It is clear that the internal friction angle in the Toyoura sand model is 5 to 6 degrees higher than that in the equivalent circles model. This mechanism can be explained as follows. Many Toyoura sand grains are in contact with each neighbor at not only single points but at two or more points, as shown in Figure 13. In the figure the lines connecting the grains indicate the contact forces and the thicker lines show larger forces than average. These plural contact points allow a transmission of the moment between the contacting grains and causes the resistance of their relative rotations. This mechanism was pointed out by Matsushima and Konagai (2001), through a simulation with regular polygonal elements.

The actual internal friction angle of dense Toyoura sand is around 50 degrees. Since the simulation presented here is 2-D, we cannot directly compare the numerical results with experimental ones.

4. Conclusion

A dynamic optimization algorithm for direct shape modeling of sand grains for the Discrete Element Method was developed and evaluated. It was found that the algorithm is valid from a relatively small number of primitive elements to large numbers of elements in both 2-D and 3-D modeling. For an accurate modeling with relatively large numbers of elements, the computation time becomes longer due to the convergence degradation that comes from the essential nonlinearity of the problem. However it is not a problem in practical sense because once the catalog of the grains model is constructed it can be used directly in a usual DEM program.

The accuracy of the modeling can be roughly estimated from the number of adopted elements in both 2-D and 3-D with a unified relation.

Using the proposed algorithm, a 2-D grain shape catalog of Toyoura sand was prepared. The adaptability into DEM of the modeled grains was verified through the bi-axial element test. The high shear strength of the specimen obtained in comparison with the equivalent circles model was discussed in relation to the transmission of the moment among the plural contact points between the grains.

5. Acknowledgment

Financial support from the Hosokawa Powder Technology Foundation, Japan is gratefully appreciated.

6. References

Cundall, P. A. (1971), A computer model for simulating progressive, large-scale movements in blocky rock systems. *Symp. ISRM, Nancy, France. Proc.*, 2: 129-136.

Ghaboussi, J. and Barbosa, R. (1990) Three-dimensional discrete element method for granular materials, 14, 451-472.

Iwashita, K. and Oda, M. (1998), Rolling Resistance at Contacts in the Simulation of Shear Band Development by DEM, Journal of Engineering Mechanics, ASCE, 124(3), 285-292.

Lin, X. and Ng, T.-T. (1997), A three dimensional discrete element model using arrays of ellipsoids, Geotechnique, 47(2), 319-329.

Matsushima, T. and Konagai, K (2001), Grain-shape effect on Peak Strength of Granular Materials, Computer Methods and Advances in Geomechanics, Desai et al. eds., Balkema, 1, 361-366.

Matsushima, T. (2001), Documentation of DEMSEG version 2.

Mirghasemi, A.A., Rothenburg L. and Matyas, E.L. (1997), Numerical simulations of assemblies of two-dimensional polygon-shaped particles and effects of confining pressure on shear strength, Soils and Foundations, 37(3), 43-52.

Muhlhaus, H.-B., Sakaguchi, H. and Moresi, L. (2001), Particle in Cell and Discrete Element Models for Granular Materials, Computer Methods and Advances in Geomechanics, Desai et al. eds., Balkema, 1, 511-518.

Ng, T.-T. (1999), Fabric study of granular materials after compaction, Journal of Engineering Mechanics, ASCE, 125(12), 1390-1394.

Rothenberg and Bathurst (1992), Micromechanical features of granular assemblies with planner elliptical particles, Geotechnique, 42(1), 79-95.

Thornton, C. and Liu, L. (2000), DEM Simulations of Uniaxial Compression and Decompression, Compaction of Soils, Granulates and Powders, Kolymbas and Fellin eds., 251-261.

Yoshida, T. (1994), Strain localization and shear banding during failure of sands, Doctoral dissertation, University of Tokyo (in Japanese).